

LearnedFTL: A Learning-based Page-level FTL for Improving Random Reads in Flash-based SSDs

Shengzhe Wang¹, Zihang Lin¹, Suzhen Wu¹, Hong Jiang², Jie Zhang³, Bo Mao¹
¹*Xiamen University*, ²*University of Texas at Arlington*, ³*Peking University*

Abstract

We present LearnedFTL, which applies learned indexes to on-demand page-level flash translation layer (FTL) designs to improve the random read performance of flash-based solid-state drives (SSDs). The first of its kind, it minimizes the number of double reads induced by address translation in random read accesses. To apply the learned indexes to address translation, LearnedFTL proposes dynamic piece-wise regression to efficiently build learned indexes. LearnedFTL also exploits the unique feature of page relocation in SSD internal garbage collection (GC), and embeds the learned index training in GC, which can minimize additional delay on normal read and write operations. Additionally, LearnedFTL employs a bitmap prediction filter to guarantee the accuracy of learned indexes' predictions. With these designs, LearnedFTL considerably speeds up address translation while reducing the number of flash read accesses caused by the demand-based page-level FTL. Our benchmark-driven experiments on a FEMU-based prototype show that LearnedFTL reduces the 99th percentile tail latency by $4.8\times$, on average, compared to the state-of-the-art TPFTL scheme.

1 Introduction

Since the last decade, SSDs have replaced traditional hard disk drives (HDDs) as the dominant storage media in diverse computing domains, including personal computers, enterprise servers, and large-scale data centers [45, 55]. The prevalence of SSDs comes from their performance superiority thanks to a series of software and hardware technology shifts. To be specific, SSDs replace the platter and spinner structures of HDDs [11, 28] with a massive number of CMOS-based NAND flash memory [11, 28], which can deliver a high level of internal I/O parallelism. Moreover, with sophisticated buffer designs and log-structured techniques [18, 29, 34, 59, 60], the SSD write performance has been significantly improved.

While the prior works have effectively addressed the write issues in SSDs, the impacts of read behaviors, especially the random reads, are overlooked. Unfortunately, random reads

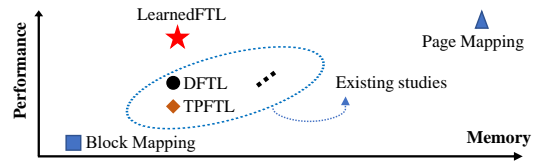


Figure 1: Performance & memory of different FTL designs.

have become a serious performance bottleneck in SSDs. It is worth noting that most applications are bonded by the read accesses [49], making the read performance critically important for SSD-based storage systems. To quantitatively analyze the problem of random reads in SSDs, we set up an experiment that executes a set of microbenchmarks on an FEMU SSD simulator [38] (cf. Section 2.1 for experiment details). Figure 2(a) shows the performance of random and sequential reads, indicating that the bandwidth of random reads only reaches up to 60% of that of sequential reads. To find out the root cause behind the performance degradation of random reads, we collect the statistics of I/O accesses and present the I/O access breakdown in Figure 2(b). Random read requests nearly double the number of flash read accesses compared to sequential read requests, in which the extra read I/Os are all used for address translation.

Address translation is a main function of flash translation layer (FTL). To be specific, modern FTL maintains page mapping information from logical pages to physical pages, that is, for a given logical page number (LPN) from the host, FTL will return its physical page number (PPN) to access the data [2, 33, 42]. However, page-level mapping requires huge memory space to store the LPN-PPN mappings. To reduce memory usage while gaining high performance, modern SSDs employ demand-based page mapping methods such as the ones in DFTL [19] and TPFTL [63]. Specifically, DFTL stores all LPN-PPN mappings in flash, and uses a small mapping cache in the SSD memory to store frequently accessed mapping information. With this mapping cache, DFTL and TPFTL can achieve excellent performance with low memory cost under workloads with high spatial and temporal locality. However, as the random reads exhibit poor data locality, the

mapping cache designs fail in accommodating the desired mapping information. As a result, almost all random read requests miss in the mapping cache. To handle a cache miss, DFTL and TPFTL need an extra flash read to bring the missing LPN-PPN mapping to the cache, which is followed by another flash read to access the data. This phenomenon is referred to *double read problem*, which is observed in Figure 2.

For further analysis, it is the locality-based cache replacement policy (e.g., LRU policy) supports the mapping cache to obtain high performance with small space. The LRU strategy needs to summarize the frequently accessed mappings from recent visits, which works well under workloads with spatial and temporal localities. However, since there is no regularity for random reads, prediction through recent visits is not feasible. As a result, caching a small part of the mapping with replacement will not work under random reads.

To solve the problem in random reads, one solution is abandoning the replacement policy and indexing almost all the mappings in cache-sized memory space, so that most random reads can be hit. Fortunately, recent studies on learned index [13, 31, 41, 56] have proved such a possibility. Learned index builds machine learning models based on the key-position mappings, thus enabling indexing hundreds of mappings with a few parameters and saving a lot of space. Ideally, by adopting the learned index to all LPN-PPNs, one can potentially calculate the PPN of an LPN directly from learned models without double reads.

However, the limitations of the learned index and the unique characteristics of flash SSD pose three challenges to its direct adoption in FTL. First, the output of any learned model is not completely accurate, what are the learned models most appropriate for FTL? Second, how to handle mispredictions? Furthermore, the learned index requires that the LPN-PPN mappings be sorted. The unique append-only and out-of-place-update characteristics of flash make such sorting impossible. Thus, the third challenge is how to obtain ordered LPN-PPN mappings in flash-based SSD.

To tackle these challenges and improve the random read performance of flash-based SSDs, we propose LearnedFTL, a learning-based page-level FTL. To solve the first challenge, LearnedFTL divides the global flash-page space into multiple partitions and fits the LPN-PPN mappings for each partition with a dynamic piece-wise linear regression (DPLR) model to achieve model accuracy. To get ordered LPN-PPN mappings, LearnedFTL utilizes the page relocation characteristics of GC to rearrange flash pages, thus generating sorted LPN-PPN mappings. Furthermore, it also proposes a novel virtual PPN representation to make the PPNs scattered under parallel units continuous. To handle the mispredictions of models, it proposes a bitmap filter to ensure the model’s correctness.

With the key challenges addressed, LearnedFTL is able to significantly accelerate address translation and reduce translation-induced double-read accesses. Figure 1 compares various types of FTL designs in terms of memory consump-

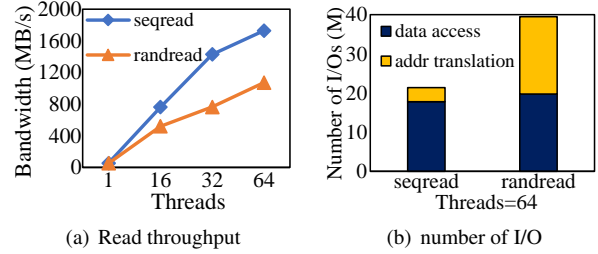


Figure 2: The performance of a FEMU-simulated SSD under sequential reads and random reads.

tion and performance. LearnedFTL achieves a performance that is close to the page-level mapping (i.e., storing the entire mapping table in memory) while preserving low memory space overhead. To the best of our knowledge, this is the first study that explores the feasibility of applying the learned index to address translation in FTL designs.

2 Background and Motivation

2.1 FTL and Address Translation

Flash memory exhibits unique characteristics, such as out-of-place updates, the erase-before-write feature, and a limited endurance [19, 22, 63]. To hide the intrinsic of flash memory and expose a block device interface to the host, flash translation layer (FTL) is employed to manage the flash memory. For incoming data, FTL simply writes the data to a free page, which is the basic unit of flash read and write, and invalidates the stale page. As a result, address mapping is required to translate a host logical page address (logical page number, LPN) to a physical flash page address (physical page number, PPN), which is called address translation. A flash block that contains several pages, is the basic unit of erase operations. When the number of free blocks decreases to a threshold, garbage collection (GC) is invoked to relocate the valid pages and erase the victim blocks.

There exist two basic address translation schemes in FTL designs [4, 32, 42] including page-level and block-level mappings. In page-level mapping, FTL maintains a fine-granule mapping table that records LPN-PPN mappings. With this fine-grained mapping, a page-level mapping scheme achieves excellent performance but requires huge memory capacity to accommodate its mapping table. For example, given an SSD of 10TB with a 4KB page size and an 8B entry for an LPN-PPN mapping, it takes 20GB memory space to store the entire 2.5 billion mapping entries in the mapping table, which is impractical in enterprise SSDs. Block-level mapping, on the other hand, records the mapping entry at the granularity of a flash block, which consumes significantly lower space overhead than page-level mapping. However, as pages can only go to fixed locations within blocks, page writing operations are limited and the performance is very poor.

To strike a good balance between performance and memory space, the state-of-the-art approaches store the entire mapping table in flash and cache only parts of the mapping table in SSD controller memory. This is referred to as demand-based page-level mapping [4]. The first such solution, DFTL [19], was proposed to exploit the temporal locality of workloads. It stores the whole mapping table in multiple flash pages, called **translation pages**, and allocates a small memory space of the controller, called **Cached Mapping Table (CMT)**, to accommodate the mapping information of several frequently accessed flash pages. The cache is usually a hash-based index with LRU-related replacement strategies. DFTL employs a **Global Translation Directory (GTD)** in the controller memory to record the physical location of the translation pages within the flash memory. However, each time the SSD controller fails in getting the mapping information of a read request from CMT, the SSD controller has to fetch the missing translation page from the flash memory by referring to GTD. This extra flash read operation is called **translation read**. Since a read request may generate two flash reads for both data and metadata, it introduces the **double-read** problem. The double-read problem significantly degrades the SSD read performance.

A series of demand-based FTLs [9, 23, 25, 50, 54, 63] have been proposed to alleviate the aforementioned double-read problem by further exploiting the locality characteristics of the workloads. One of the most famous representatives, TPFTL [63] proposes two prefetch schemes including request-level prefetch and selective prefetch. With these two prefetch techniques, TPFTL can predictively prefetch several consecutive LPN-PPN mapping entries when TPFTL reads an LPN-PPN mapping. TPFTL makes full use of the spatial locality within the workload, which greatly alleviates the double-read problem in sequential reads. However, it is non-trivial to resolve the double-read problem for random reads, which will be explained shortly.

2.2 Performance Impact of Double Reads

To investigate how the double read degrades the performance of random reads, we conduct an evaluation on TPFTL-based FEMU SSD [38] driven by microbenchmark (i.e., random and sequential reads) under different numbers of threads. As shown in Figure 2(a), no matter the number of threads varies, the performance of random reads is always lower than that of sequential reads (i.e., up to 60% degradation). We also collect the number of flash I/Os used for data reads (denoted as *data access*) and translation reads (denoted as *addr translation*) under 64 threads. As shown in Figure 2(b), almost all random reads require extra translation reads, that is, random reads in demand-based FTL frequently invoke double reads, which worsens the performance.

To figure out the reasons behind these performance results, we also conduct the same experiments with various FTL de-

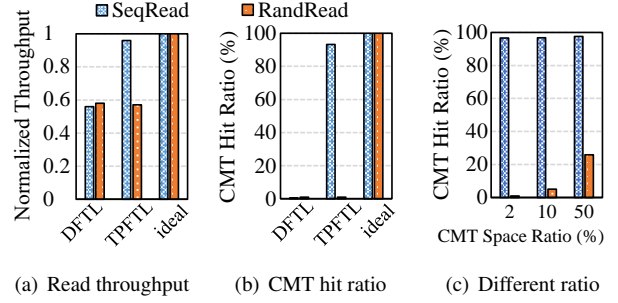


Figure 3: The performance of demand-based FTLs and ideal page-level FTL under sequential reads and random reads.

signs: DFTL, TPFTL and ideal FTL. We assume that ideal FTL stores the entire page mapping table in memory. Figures 3(a) and 3(b) show the read throughput and the CMT hit ratio in a single-threaded environment. First, Figure 3(a) shows that TPFTL achieves similar throughput as the ideal FTL under sequential reads. This is because TPFTL exploits the spatial locality in sequential reads to significantly reduce the number of translation reads, which in turn achieves a 93% CMT hit ratio. By contrast, DFTL exploits only the temporal locality in sequential reads, which is ineffective with a 0% CMT hit ratio. This enforces DFTL to fetch the mapping information from the underlying flash for each read I/O, thus incurring more double reads. Second, both DFTL and TPFTL perform poorly in random reads, which is at a level much lower than the ideal FTL. As shown in Figure 3(b), the CMT hit ratios are almost 0 (0.1% for DFTL and 0.09% for TPFTL), which means that the read amplification is almost 2. These results indicate that double reads occur for nearly all random read requests.

One simple way to improve random read performance is to increase the size of the CMT. However, this solution still performs poorly due to the contention of the memory cache. Figure 3(c) illustrates the changes in TPFTL’s CMT hit ratio when increasing CMT space. The hit ratios of random reads are only 1%, 5%, and 25.9% when the CMT sizes are set as 2%, 10%, and 50% of the total mapping table size, respectively. It is evident that, as long as CMT cannot accommodate the vast majority of the mappings, the contention for CMT will not disappear. As a result, for any practical capacity of the CMT, the prefetched mappings will be replaced frequently and cause a low CMT hit ratio.

The root cause of why CMT cannot handle random reads comes from its locality-based cache replacement policy, which employs least recently used (LRU) strategies. This policy can identify the locality of workload, and retain the frequently accessed mappings in the cache. That’s why it can handle the sequential reads well. However, as there is no frequently accessed mappings under random reads, the LRU policy fails to retain the correct mappings. As a result, the very few mappings that reside in the cache are rarely hit, thus incurring more double reads. What’s worse, this policy can

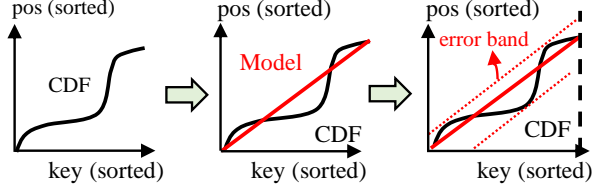


Figure 4: The workflow of the learned index.

also incur fierce competition for cache space, which makes its hit ratio even lower. The above analysis demonstrates that small-capacity caches relying on efficient replacement strategies cannot handle the address translation in random reads.

2.3 Learned Index and Challenges of Applying It to FTL Designs

Since a random read request may access any LPN in the entire logical address space, an efficient solution is to place as many mappings as possible in the cache-sized SSD memory space. For example, if the FTL can index 50% of the mappings in the cache-sized space, it can reduce double reads by 50% in the random read requests. Fortunately, the space-efficiency **learned index** [13–15, 31, 40] has proved such a possibility. Learned index builds lightweight models for key-position mappings. Hundreds of data locations can be calculated by a model with several parameters, thus reducing memory consumption. Figure 4 illustrates the workflow of the learned index. The main target of the learned index is to train an approximate model (usually a straight line) over the key-position mappings with an error band to make sure that all data are in the interval $[y_{predict} - error, y_{predict} + error]$. The workflow consists of the following three steps: sort the keys in increasing order and place them in sequential physical locations (pos) (❶); train predefined model over the $\langle key, pos \rangle$ pairs (❷); use all the $\langle key, pos \rangle$ pairs as the input of the model to calculate the maximum error band of both the predicted value and the true value (❸). Moreover, since the positions of keys may be updated, the model must be periodically retrained.

The aforementioned workflow shows three essential requirements for applying the learned index in FTL. Firstly, it is essential to group the training data and select a proper model. Secondly, the *key* in $\langle key, pos \rangle$ pairs must be sorted, and the *pos* in $\langle key, pos \rangle$ pairs must be contiguous to guarantee the accuracy of the approximate model. Lastly, an error interval is in need to guarantee 100% correctness.

Ideally, applying learned index to the demand-based FTL would be a solution to accelerate random reads. By applying the learned index to all LPN-PPN mappings, FTL can calculate the PPNs with the learned models for the LPNs missed from the CMT, thus avoiding the extra flash read for the missing mapping information. However, before applying the learned index to the page-level mapping FTL, we need to examine whether the flash-based SSDs and DFTL meet the aforementioned three requirements of the learned index.

To satisfy requirement (1) in flash-based SSDs means deciding how to group LPN-PPN mappings for learned models and what model should be used within each LPN-PPN group. Since each entry in the GTD is linked to a translation page containing a range of contiguous LPNs and their mapped PPNs (cf. Figure 5). The best way of employing the model is to build learned models for each GTD entry. Therefore, the first challenge is to choose an appropriate model, that is, **what kind of learned model is the most suitable?**

To satisfy requirement (2) means that both LPNs and PPNs in each LPN-PPN group must be sorted in order. However, due to the unique characteristics of flash-based SSDs (i.e., append-only and out-of-place update), the mapped PPNs of contiguous LPNs are usually distributed in random and non-contiguous physical space. Even though GTD is organized based on orderly and contiguous LPNs, the mapped PPNs of each GTD entry may be unordered and incontiguous after SSD writes. To make things worse, the SSD internal parallelism and dynamic allocation strategies force flash pages in different flash channels to be scattered further. Therefore, the second challenge is, **how can we reorder the mapped PPNs of contiguous LPNs?**

To satisfy requirement (3) means using an error interval to make the model output accurate. However, using an error interval to guarantee 100% correctness generates more flash reads. Specifically, since there is an error interval in the model predictions, multiple pages in the error interval need to be read from NAND flash so as to obtain the correct translation page, which severely worsens the read performance. As the goal of this work is to improve random read performance, therefore, the third challenge is, **how can we determine the correctness of a predicted PPN in the learned model?**

Recent advances in the learned index have shown that it can achieve significantly faster lookup times and index space savings [15, 31]. Motivated by the urgent need to resolve the double-read problem caused by random reads in flash-based SSDs, we propose LearnedFTL, which uses lightweight learned models, low-cost model training via GC, and a precise prediction filter, to accelerate the random-read performance in flash-based SSDs.

3 LearnedFTL

3.1 System Overview

The main idea of LearnedFTL is to use learned index models to predict the PPNs when I/O requests miss from the CMT, thus reducing the number of double reads induced by random read requests. Figure 5 illustrates the system overview of LearnedFTL, which adopts a demand-based FTL framework [19, 63]. Based on the analysis in Section 2.3, a model layer is introduced into the Global Translation Directory (GTD) for mapping prediction. Each GTD entry has a specific learned index model. For LPNs that miss the CMT, the learned index

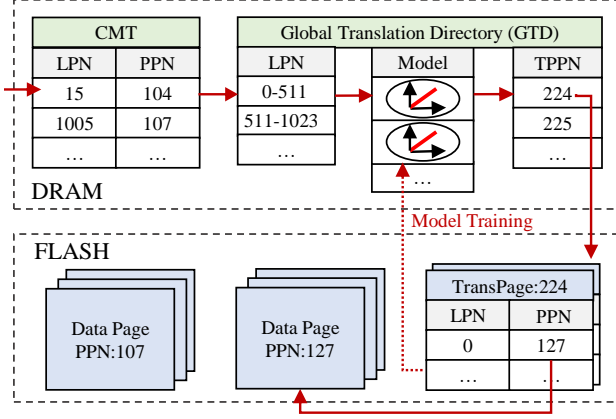


Figure 5: The system overview of LearnedFTL.

models can predict the PPNs. Each time a PPN is correctly predicted, the corresponding double read is eliminated.

Each GTD entry is associated with a dedicated learned model. An entry in GTD indexes a translation page (TransPage in Figure 5, indexed by translation PPN in GTD, denoted as TPPN) that stores hundreds of LPN-PPN mappings (e.g., 512 for an SSD with a page size of 4KB and PPN size of 8 Bytes). It is worth noting that such a number of mappings is compatible with the state-of-the-art Learned Indexes [13, 31, 40] that usually build a learned model for hundreds of key-value pairs, making a GTD entry a sensible basic unit to build a learned model.

To solve the challenge of model selection, LearnedFTL uses a Dynamic Piece-wise Linear Regression model to achieve high accuracy and high space efficiency (cf. Section 3.2 for details). To solve the challenge that how to obtain contiguous LPN-PPN mappings, LearnedFTL uses a method of Low-cost Model Training via Garbage Collection (GC) by Group-based Allocation and Virtual PPN Representation (cf. Section 3.3 for details). To solve the challenge of how to determine the correctness of model prediction, LearnedFTL uses a Bitmap Filter method to filter the correct model predictions (detailed in Section 3.4). With Bitmap Filter, LearnedFTL solves the challenge of how to determine the correctness of the predicted PPN.

3.2 Dynamic Piece-wise Linear Regression

The knowledge about the data to be trained is important for the model selection. To this end, we collect several GTD entries' valid LPN-PPN mappings in DFTL with stable state. To make the mappings meet the requirement(2) in Section 2.3, we reallocate contiguous PPNs. Figure 6 shows the typical image of LPN-PPN mappings, where we label different segments of contiguous LPN-PPN mappings (i.e., both LPN and PPN are contiguous) with different colors. These disconnected segments (i.e., short straight lines) collectively form a roughly straight line. This suggests that a proper choice is the piece-

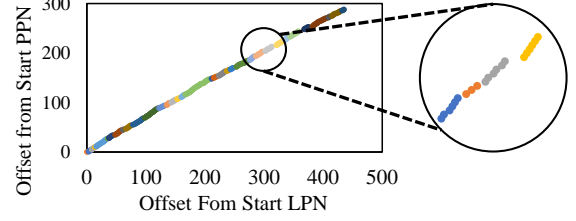


Figure 6: An example for LPN-PPN translations. Each color represents a contiguous segment.

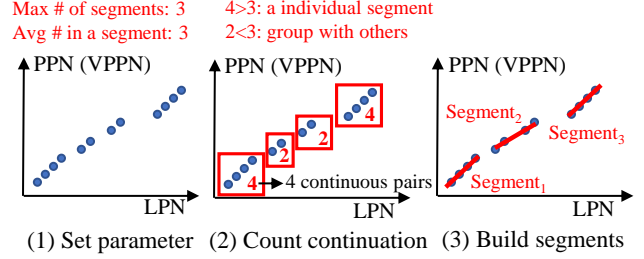


Figure 7: The process of DPLR building.

wise linear regression (PLR) model if all contiguous segments of a GTD entry can be fitted with linear regression.

However, the number of locally contiguous LPN-PPN mappings may be too large (36 segments in Figure 6) to assign a model for each segment. Considering space footprint, the best solution is to preferentially fit an individual model for the longest continuous segments, thus ensuring high accuracy.

To this end, we propose a **dynamic piece-wise linear regression (DPLR)** to achieve high model accuracy with fewer segments. In DPLR, the maximum number of segments is set as N (typically 8 but can be adjusted according to the environment), which means that there are at most N linear regressions. Supposing there are M LPN-PPN mappings, DPLR fitting needs three steps, as shown in Figure 7: (1) Set Parameters: LearnedFTL first sets the average length of each segment by M/N . If the length of one continuous LPN-PPN mapping exceeds this average value, these mappings can form one individual segment with a linear model (called **Large Segment**). (2) Count continuation: LearnedFTL traverses all mappings and records all large segments. Supposing there are T large segments, the remaining mappings are combined into $N-T$ segments as close as possible. (3) Build segments: LearnedFTL performs the Least Squares algorithm [6] to calculate the parameters of linear models.

After all the segments are processed, their metadata are combined, including the slope k , intercept b , and the offset off of each segment from the start LPN. Then these metadata are updated to the model layer of the corresponding GTD entry. Figure 8 shows the data structure of an entry's model layer in GTD. Besides the segment metadata, DPLR models also store the *start_PPN* to indicate the start PPN of the LPN-PPN mappings in the group, a bitmap with M bits to filter predictions (cf. Section 3.4). Since each GTD entry uses the start LPN as an index, it is not stored in the model layer.

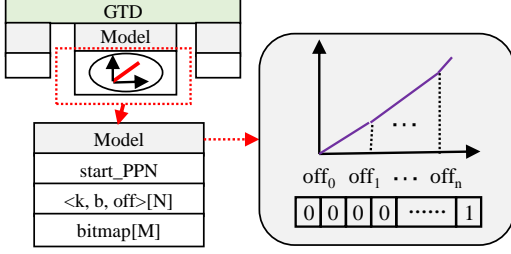


Figure 8: The data structure of a model in a GTD entry.

LearnedFTL proposes **sequential initialization** to make the DPLR model efficient before GC. The sequential initialization happens when GTD is built. For each GTD entry, the model is initialized to $y = x$, where all bits in the bitmap are set to 0, and the *start_PPN* is set to *NULL*. When the first write request with contiguous LPNs arrives in the SSD, *start_PPN* is set to the first assigned PPN of these LPNs. Then LearnedFTL sets the remaining bits corresponding to these contiguous LPNs to 1.

3.3 Low-Cost Model Training

We propose a new technique, called low-cost model training, to address the PPNs-reordering issue (i.e., how to reorder mapped PPNs of contiguous LPNs). Since the flash-based SSDs need to perform garbage collection (GC) to relocate the valid pages, it provides us an opportunity to rearrange the physical location of the data to make them in the desired order. As a result, it is possible to collect the valid pages with LPNs of one GTD entry, sort these LPNs in order, and write them back in contiguous PPNs. The sorted LPNs in increasing order and contiguous PPNs are then used to train the DPLR models detailed in Section 3.2. This, however, hinges on whether LearnedFTL can address the two challenges described in Section 2.3, i.e., (1) How to reorganize the random PPNs caused by the allocation strategy? and (2) How to ensure the PPNs are contiguous without affecting the access parallelism?

3.3.1 Group-based Space Allocation

The high complexity of PPNs-reordering stems from the SSD’s space allocation strategy, that is, it assigns LPNs their corresponding PPNs [22, 38]. The mainstream page allocation strategy is dynamic allocation [22, 38]. In this strategy, when an LPN needs a physical page, the FTL will select the least busy flash chip (the parallel unit in SSD to execute requests) to allocate pages so as to achieve the best parallelism and write efficiency.

However, with dynamic allocation, the PPNs of a GTD entry will be scattered in various locations. When building a learned model over this GTD entry, it is necessary for the GC process to collect the valid pages across multiple flash blocks, and these blocks also contain data (PPNs) belonging to multiple GTD entries. As a result, the GC process needs a

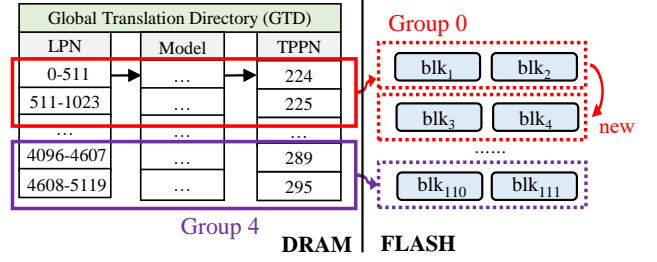


Figure 9: An example of group-based allocation.

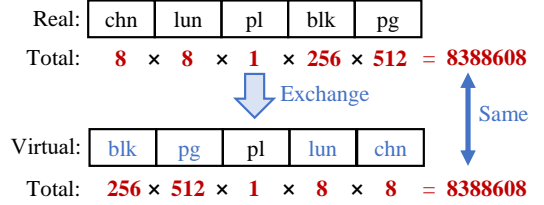


Figure 10: The principle of virtual PPN translation.

large amount of data movement, which significantly increases the complexity and overhead of the model training process.

To address this issue, we propose a group-based allocation strategy in our LearnedFTL to reduce the GC overhead and simplify the model training [5]. The basic idea is to divide GTD into groups of consecutive entries, referred to as *GTD entry group*. Each group is allocated with an exact number of contiguous flash blocks to accommodate all the LPNs of the group. When the flash blocks allocated to a GTD entry group are full, these used flash blocks are replaced by the same number of contiguous empty flash blocks. When there are no empty flash blocks or the cumulative number of flash blocks allocated to this GTD entry group reaches a threshold, GC is performed on the GTD entry group with the most invalid data pages. During GC, LearnedFTL reclaims data blocks by relocating the valid data pages and retrains the learned models for all GTD entries in this group.

Figure 9 illustrates an example of group-based allocation. In this instance, for the convenience of presentation, each GTD entry group contains two entries and needs two contiguous flash blocks to accommodate all its LPNs. Therefore, LPNs 0-1023 belong to group 0 and LPNs 4096-5119 belong to group 4. When a request for data with LPN belonging to group 0 arrives, two contiguous blocks, *blk1* and *blk2*, are allocated to group 0. When a request for data with LPN belonging to group 4 arrives, another two contiguous blocks, *blk110* and *blk111*, are allocated to group 4 to accommodate the required data pages. When group 0 has no free physical pages, another two contiguous blocks, *blk3* and *blk4*, are allocated to this group. If group 0 is selected for garbage collection, all four blocks are collected directly.

3.3.2 Virtual PPN representation

The second challenge of non-contiguous PPNs stems from the write-back stage in the GC process. When the valid sorted

	①	②	③	④	⑤	
LPN	chn	lun	pl	blk	pg	True PPN
1001	4	5	1	64	127	= 5013631
1002	5	5	1	64	127	= 6062207
1003	6	5	1	64	127	= 7110783

↓

	①	②	③	④	⑤	
LPN	blk	pg	pl	lun	chn	Virtual PPN
1001	64	127	1	5	4	= 2105388
1002	64	127	1	5	5	= 2105389
1003	64	127	1	5	6	= 2105390

Figure 11: An example of PPN-to-VPPN translation.

pages collected by GC need to be written back, they must be written back in contiguous PPNs. However, the pages in multi-channel SSDs may be written back to different flash chips, leading to non-contiguous PPNs.

To tackle this problem, LearnedFTL uses a virtual PPN (VPPN) representation that aims to transform the non-contiguous PPNs scattered across different chips into contiguous ones. This translation thus allows LearnedFTL to build a model based on contiguous LPN-VPPN pairs. When predicting the PPN of an LPN, LearnedFTL first uses this LPN to predict the VPPN and then translates this VPPN to PPN to get the physical address to complete the prediction.

Figure 10 shows the principle of translation from PPN to virtual PPN. Since the total number of physical flash pages is fixed in an SSD, the PPN is formed in such a way that it represents the hierarchical tree structure of an SSD by the concatenation of address fields representing different levels of the hierarchy from the highest (channel) to the lowest (page) granularity. Because of the commutative law of multiplication, the order of these address fields in PPN can be changed to obey the allocation order. After the change, each physical page retains its unique number, and the new page number will become contiguous according to the allocation order.

Figure 11 gives an example of the PPN-to-VPPN translation. In LearnedFTL, the allocation order is *channel, chip, plane, page, and block*, which is the fastest allocation order based on the previous study [22]. For requests with LPNs 1001, 1002, 1003 that are already written to flash-based SSD, their PPNs are 5013631, 6062207, 7110783, which are not contiguous. However, after the PPN-to-VPPN translation by changing the order of the fields in the address appropriately, LearnedFTL obtains contiguous VPPNs 2105388, 2105389, 2105390 for these LPNs.

The virtual PPN representation allows LearnedFTL to generate contiguous VPPNs for model training when valid pages are written back to the flash-based SSDs concurrently. Since the training model is built based on LPN-VPPN mappings, the predicted VPPN needs to be translated back to PPN to obtain the physical flash page.

3.3.3 Model Training Process with GC

When a GTD entry group needs to perform GC, the whole model training process via GC is divided into three steps:

① **Regulate valid translations.** First read all the translation pages of this GTD entry group and only keep the valid translations in memory. Then sort the valid translations by their LPNs to make them ordered.

② **Write valid data back and obtain VPPNs.** First allocate another group of flash blocks to this GTD entry group. Then write the valid pages back to the newly allocated flash blocks. For each GTD entry in this GTD entry group, calculate the VPPNs corresponding to the new PPNs, and combine the VPPNs and LPNs for the training dataset.

③ **Train the learned model.** In this step, each GTD entry in this group will train its own DPLR model. For each GTD entry, calculate the offset of VPPNs/LPNs from this GTD entry's starting VPPN/LPN. Then, perform DPLR model fitting to get the <slope, intercept, offset> model arrays. Finally, evaluate the accuracy of the model and update the bitmap filter (detailed in Section 3.4).

3.3.4 Model Training within Rewrite

For some scenarios where GC rarely happens, the model training can be integrated into the SSD rewrite process [8, 43]. The rewrite is a widely used reliability mechanism to reduce retention errors in modern SSDs by periodically reading, correcting, and reprogramming the flash memory. Rewrite happens frequently and is the most significant factor for write amplification [43]. During SSD rewrite, LPNs of flash pages can be sorted in order so that these pages are written back in contiguous PPNs, which then enables a model to be built and trained on them by LearnedFTL.

3.4 Bitmap Prediction Filter

The bitmap prediction filter is designed to address the third challenge (i.e., how to determine the correctness of a model PPN prediction). Since it is impossible to achieve 100% accuracy without an error interval, a fail-safe solution is to perform double reads to fetch the correct data page on the unmatched PPNs. As a result, a prediction filter is needed to confirm whether a requested LPN can predict accurately.

LearnedFTL uses a bitmap data structure to filter the correct predictions called the bitmap prediction filter. For each LPN in an SSD, LearnedFTL assigns one bit to indicate whether it can predict the real PPN for this LPN. As illustrated in Figure 8, for a GTD entry with M LPNs, LearnedFTL assigns a bitmap with M bits for all LPNs. During the LPN-PPN translation, when an LPN cannot hit in CMT, LearnedFTL will check this LPN's bit in the bitmap, that is, check whether the corresponding bit is 1. If yes, it means the model prediction with this LPN is trusted. Then LearnedFTL can directly use the corresponding linear model to calculate the VPPN, translate

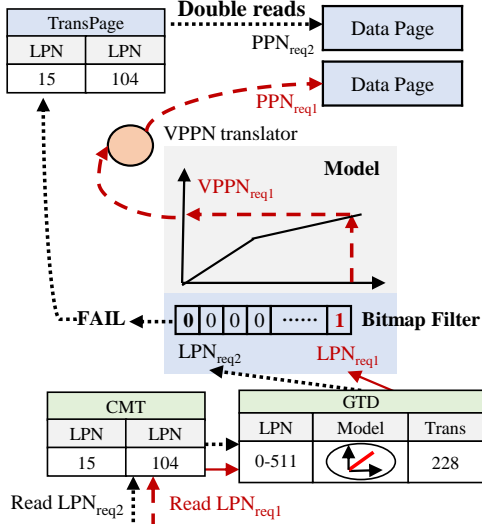


Figure 12: The workflow of bitmap prediction filter.

the VPPN to PPN, and use the PPN to access the data page. If the bit is 0, LearnedFTL will perform a double read for this LPN and will not use the model to make predictions. With the bitmap prediction filter, LearnedFTL can make only the correct model predictions and avoid miss penalty caused by wrong model predictions. Figure 12 illustrates two different instances of the bitmap prediction filter.

The bitmap prediction filter is built in the model evaluation process (step 3 in Section 3.3). After one DPLR model is trained, all valid LPNs of this GTD entry are input to the trained model to get the predicted PPN. If the predicted PPN is consistent with the real PPN, this LPN corresponding bit in the bitmap is marked as 1. Otherwise, it is marked as 0.

The data consistency of the bitmap is guaranteed upon each update. For each write request with an LPN, LearnedFTL will first check if the corresponding bit of this LPN in the bitmap is 1. If yes, LearnedFTL will set this bit to 0. Since persisting the bitmap in NAND flash with each update will incur significant performance overhead, LearnedFTL chooses not to persist them in SSD until a normal power off or rebuild the bitmap by scanning on a power failure as TPFTL and DFTL do.

3.5 Cost Analysis

Though LearnedFTL introduces multiple new components to apply the learned index in the FTL, it only introduces minor computational overhead compared to DFTL and TPFTL. We discuss the details as follows.

(1) Read: For each read request with an LPN, LearnedFTL incurs two additional operations when this LPN cannot hit in the CMT. The first operation is a **bitmap check** to check if this LPN can predict a real PPN. The second operation is a **model prediction** when the answer of the bitmap check is yes. For these LPNs, LearnedFTL will use the model to predict the real PPN instead of an extra flash read. The model

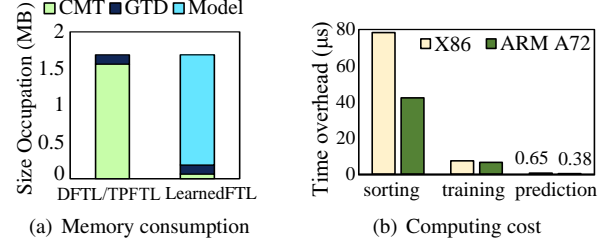


Figure 13: The memory consumption and computing cost of the additional operations between ARM and X86 processors.

prediction includes calculating the VPPN with the $y=kx+b$ model and translating the predicted VPPN to PPN.

(2) GC: The model training incurs two computational overheads during the GC period. The first one is **sorting** all the LPNs within each GTD entry (Step ① in Section 3.3.3). The second one is **training** each GTD entry's model (Step ③ in Section 3.3.3).

Our experiments in Section 4.3 have detailed evaluations to quantitatively analyze these overheads.

4 Performance Evaluation

4.1 Implementation and Experiment Setup

Experiment Setup: The experiments are conducted on FEMU [38]. FEMU is a QEMU-based and DRAM-backend SSD emulator that is widely used in recent studies [20, 39, 64]. It runs in a machine with two Intel(R) Xeon(R) Gold 5318Y 2.10GHz CPUs and 128GB DRAM. The operating system is Linux with kernel version 5.4.0. The emulated SSD is configured with 32GB logical capacity plus 2GB over-provisioning space and has 64 parallel chips (8 channels and 8 ways per channel). Each flash chip has 256 flash blocks and each flash block has 512 flash pages. The size of a flash page is set to 4KB. The latency of NVMe SSD is 40 μ s for NAND read, 200 μ s for NAND write, and 2ms for NAND erase, which are the default settings in FEMU and widely used in the recent flash-based studies [20, 38, 39]. Since the SSD rewrite for retention errors is not implemented in FEMU [43], we only train models in GC.

LearnedFTL is compared against two representative page-level FTL designs, DFTL [19] and TPFTL [63]. We also use full-page mapping as a control (denoted as *ideal*, which is considered a performance upper bound). In the experiments, we use both FIO benchmark [24] and real-world applications/traces to evaluate different FTL designs.

Prototype implementation: We implement LearnedFTL by modifying the blackbox mode of the FEMU based on the TPFTL scheme. The CMT has 8192 slots which are about 0.1% of the total flash pages. According to the allocation strategy and internal parallelism of the SSDs, we group each 64 consecutive GTD entries as a *GTD entry group*. Since the size of a flash page is 4KB and each translation page has

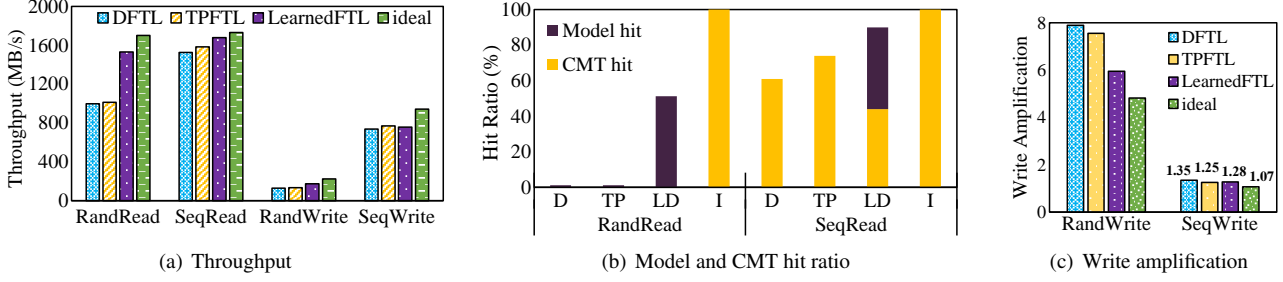


Figure 14: The performance results of FIO benchmark under 64 threads (D: DFTL, TP: TPFTL, LD: LearnedFTL, I: ideal FTL).

512 LPN-PPN mappings, the GTD has 16384 entries. Each GTD entry group is allocated 64 flash blocks at a time, one for each of the 64 translation pages. For parameter setting in the piecewise linear model, 8 pieces are set by default.

Since the previous demand-based FTLs, such as DFTL and TPFTL, are implemented on trace-driven simulators, such as SSDsim [22] and Flashsim [30], we incorporate them into the FEMU emulator according to their designs in the papers. For their allocation strategy, we use FEMU’s default greedy dynamic allocation strategy. We added and modified about 4,000 LoC to implement these baselines and the LearnedFTL in FEMU. The source code of these prototype implementations, along with our LearnedFTL on the FEMU platform, will be released upon the publication of the paper.

Memory consumption: LearnedFTL adds a model layer in GTD on the basis of TPFTL, which brings additional memory space overhead. In LearnedFTL, each model has three parameters, $start_PPN$, $\langle k, b, off \rangle [N]$ and $bitmap$. For $start_PPN$, LearnedFTL stores it as a `uint64_t` integer. For $\langle k, b, off \rangle [N]$, each integer is a type of `uint8_t` to save space. For $bitmap$, each slot is a bit, which makes the bitmap the biggest memory space overhead. To sum up, a model in a GTD entry requires 96 Bytes. For a fair comparison, we increase the CMT size in DFTL and TPFTL to ensure the same memory space overhead as that of LearnedFTL. Figure 13(a) illustrates the total memory consumption of DFTL, TPFTL, and LearnedFTL.

Controller computing: Since LearnedFTL adds some additional computing operations mentioned in Section 3.5, it is necessary to correctly simulate the computing power of the SSD controller. The mainstream SSD controller CPUs are ARM’s Cortex A series and Cortex R series. we compared the time consumption of executing the additional operations on the FEMU simulated CPU (X86) and a low-end embedded processor (ARM Cortex-A72) and each operation is at the maximum complexity. Figure 13(b) shows that the ARM A72 processor even performs better than the X86, which shows that we can use the X86 FEMU simulator to simulate LearnedFTL’s computing power.

4.2 FIO Benchmark

We first use the FIO benchmark [24] to evaluate the performance of sequential writes, random writes, sequential reads, and random reads for different FTL designs.

(1) Read: For random-read and sequential-read evaluations, we first perform 10 minutes of FIO random writes to warm up the whole SSD, then we perform a corresponding FIO read benchmark for 5 minutes. All the above benchmarks use 4KB I/O size and *psync* I/O engine with 64 threads.

Figure 14(a) illustrates the throughput results for different FTL designs under different access patterns. For random read, LearnedFTL outperforms DFTL and TPFTL by $1.5\times$ and $1.4\times$, respectively. For sequential read, LearnedFTL outperforms DFTL and TPFTL by $1.1\times$ and $1.1\times$, respectively. Moreover, the performance of LearnedFTL is very close to that of the ideal FTL, achieving about 89.2% and 96.8% of the performance of the ideal FTL under random reads and sequential reads, respectively.

To explore the behind reasons, we also recorded the percentage of requests that hit the CMT and the learned models during random and sequential reads. The ideal FTL is used as a control which can be considered as an upper bound since its CMT has a hit ratio of 100% and infinite space.

Figure 14(b) shows that the CMT hit ratios of DFTL and TPFTL designs are almost 0 under random reads. The reason is that random reads show no locality, which makes the cache replacement policy fails to capture the access pattern. By contrast, LearnedFTL utilizes the low-cost learned models to index most of the mappings, achieving 55.5% hit ratios in the models, which reduceing 55.5% extra flash translation reads. As a result, LearnedFTL significantly improves the random-read performance over DFTL and TPFTL.

Under sequential reads, LearnedFTL still outperforms DFTL and TPFTL. Although DFTL and TPFTL respectively achieve 61% and 80% hit ratios on CMT, their CMT hit ratios are quite different in a single-threaded environment shown in Figure 3(b). The reason is that the throughput of DFTL and TPFTL can be affected by parallel threads which in turn affect the locality of sequential reads (i.e., increasing temporal locality but decreasing spatial locality). Driven by parallel threads, the space contention in the CMT may cause some

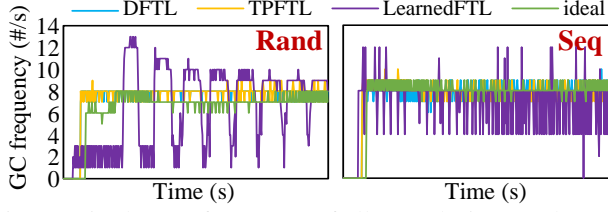


Figure 15: The GC frequency of all FTL designs under FIO random and sequential write benchmarks.

misses, resulting in a lower CMT hit ratio.

By contrast, LearnedFTL can resolve contentions effectively. Compared to the mapping entries in the CMT, the learned models have a much longer life cycle because they are only rebuilt during GC periods and will not be evicted as the mapping entries in the CMT. As a result, LearnedFTL achieves a combined CMT-Model hit ratio of up to 90%, eliminating 90% of the LPN-PPN double reads. Thus, LearnedFTL achieves the best performance among all FTLs and approaches that of the ideal FTL, which is the upper bound.

(3) **Write:** For the random-write and sequential-write evaluations, we perform a corresponding write benchmark in FIO for 10 minutes from the empty state of SSD, and all the evaluations use 4KB I/O size and *psync* I/O engine with 64 threads.

Figure 14(a) shows that under random writes, LearnedFTL outperforms DFTL and TPFTL by $1.4\times$ and $1.2\times$, respectively, because of LearnedFTL’s group-based allocation strategy. Since LearnedFTL selects a GTD entry group for each GC, only the translation pages of this GTD entry group need to be updated. That is, a maximum of 64 translation pages are updated per GC. However, for the dynamic allocation strategies used in DFTL and TPFTL, when the same number of data blocks are collected, the LPN range of flash pages written back may be more than 64 translation pages, which causes additional write amplification.

Owing to the spatial locality of sequential writes, LearnedFTL performs almost the same as DFTL and TPFTL, by less than 2%. Unlike the dynamic allocation strategy which selects the blocks with the fewest valid pages in each GC, the group-based allocation strategy performs GC on a group-by-group basis, which may result in more valid pages being written back. But the result shows that this does not have a large impact on sequential write performance.

4.3 Overhead Analysis

LearnedFTL added additional operations to SSD. In this subsection, we evaluate the overhead induced by these operations.

(1) **GC frequency and write amplification:** In LearnedFTL, model training happens in GC, and LearnedFTL proposes group-based allocation to assist model training. Therefore, the GC frequency and write amplification are critical indicators. Figure 15 illustrates the GC frequency of various FTLs in the FIO write evaluations. Although the

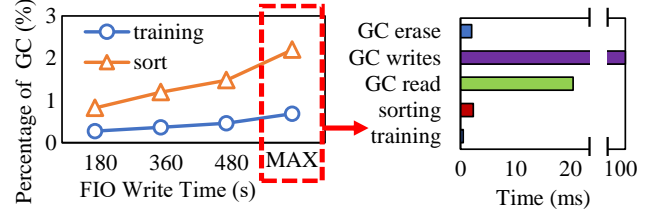


Figure 16: The time overhead of sorting and training under different running times of FIO random writes (MAX means almost all pages are valid during GC).

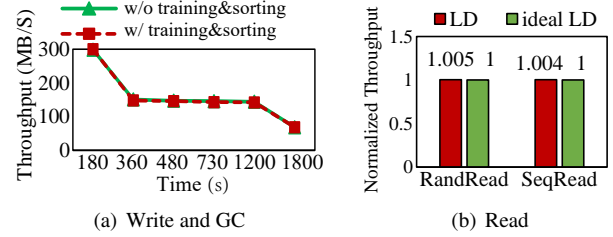


Figure 17: Performance of LearnedFTL with and without additional computing operations (LD: LearnedFTL, ideal LD: ideal LearnedFTL)

GC frequency of LearnedFTL fluctuates, the total number of GCs triggered under random writes and sequential writes of LearnedFTL (4188 and 4285) are less than DFTL (4335 and 4572) and TPFTL (4335 and 4304). Figure 14(c) also shows that the write amplifications of DFTL and TPFTL are larger than LearnedFTL in random writes because the group-based allocation requires fewer translation page writes. For sequential writes, although the group-based allocation may write more valid pages, the write amplification of LearnedFTL is comparable to DFTL and TPFTL. Overall, our group-based allocation can effectively assist the learning models without causing additional GC and write amplification.

(2) **Overhead of training and sorting:** The **model training** (denoted as training) and **PPNs-sorting** (denoted as sorting) are two additional operations added to GC. In our implementation, we group 64 GTD entries into one group. In one GC, a maximum of 64 PPN-sorting and model training operations will be triggered for one GTD entry group. As mentioned in Figure 13(b), each GTD entry needs about $50\mu s$ for sorting and training in ARM Cortex-A72. The maximum additional overhead incurred by sorting and training are equivalent to about 80 SSD reads (μs per read), which is negligible since GC for one GTD entry group will incur tens of thousands of SSD reads and writes. Figure 16 show that the time consumption of training and sorting only accounts for up to 3.2% of the GC execution time.

GC and write requests do not block each other. To further explore whether they will introduce additional latency, we compare FIO random write performance of LearnedFTL with and without these additional operations. Figure 17(a) shows that their performance difference is nearly negligible (less

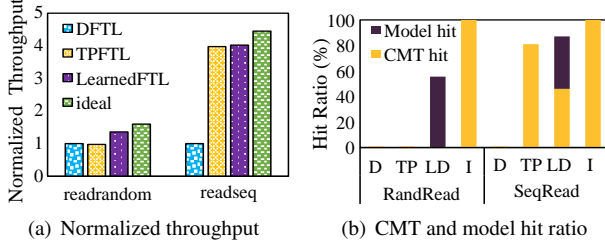


Figure 18: Performance results of RocksDB with one thread (D: DFTL, TP: TPFTL, LD: LearnedFTL, I: ideal FTL).

than 0.7%), further verifying that the computing overhead of training and sorting is minimal in LearnedFTL.

(3) Overhead in read operations: As mentioned in Section 3.5, only LPNs that can be correctly predicted will perform **model prediction** ($0.65\mu s$ in Figure 13(b)). This means there is no miss penalty in model predictions. Although there is no miss penalty, if the model prediction takes too long, it will reduce the advantage of reducing double reads. We implement ideal LearnedFTL which put all mappings in memory. For ideal LearnedFTL, each time the bitmap check is yes, it can directly get the PPN through mapping table without model prediction. Figure 17(b) shows that the FIO read performance gap between LearnedFTL and ideal LearnedFTL does not exceed 1%, demonstrate that the model predictions are lightweight.

4.4 Real-World Applications

We use Filebench [16] and RocksDB [52] as two real-world applications to evaluate the efficacy of different FTL designs.

RocksDB: RocksDB [52] is a widely used LSM-Tree-based KV store designed to exploit the parallelism of flash-based SSDs. As we mentioned before, LSM-Trees can merge random writes into sequential ones, but at the cost of relatively poor services to random reads. We deploy RocksDB with EXT4 file system on top of each FTL design and use the *db_bench* tool of RocksDB with one thread, which is consistent with the previous studies [27, 51, 58]. To evaluate the read performance, we first use the *fillseq* and *overwrite* in *db_bench* to write the DB to 80% full, then we perform *readrandom* and *readseq* in *db_bench* to evaluate the read performance in RocksDB.

In terms of throughput, Figure 18(a) illustrates that LearnedFTL outperforms DFTL and TPFTL by $1.3\times$ and $1.3\times$ in random reads. LearnedFTL also outperforms DFTL and TPFTL by $1.7\times$ and $1.02\times$ in sequential reads.

To better understand these results, Figure 18(b) shows the model and CMT hit ratios recorded in these evaluations. In a single-threaded environment, DFTL does not exploit and thus fails to benefit from the spatial locality, so its CMT hit ratio is zero. TPFTL can achieve an 81% CMT hit ratio by exploiting the spatial locality. By contrast, since LearnedFTL exploits both the spatial locality and the learned model, it achieves

Table 1: Filebench configurations.

Name	Fileset	Feature	Threads
fileserver	$22,500 \times 128KB$	write heavy	50
webserver	$82,500 \times 16KB$	read heavy	64
randomread	$24,000 \times 1MB$	all read	64

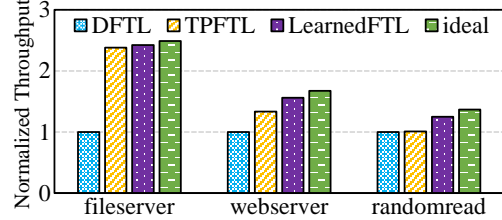


Figure 19: The normalized throughput of Filebench.

0.3% and 46% CMT hit ratio, 55% and 41% model hit ratio in random reads and sequential reads, respectively.

Filebench: *Filebench* [16] is a highly flexible storage benchmark. We select three workloads that are most widely used in previous studies [7, 20, 64]: *fileserver* (write heavy), *webserver* (read heavy, less random write), and *randomread* (all random reads). Their configurations, consistent with previous studies [20, 64], are summarized in Table 1.

Figure 19 shows that LearnedFTL outperforms DFTL by $2.4\times$, $1.5\times$, and $1.2\times$ under the three workloads, respectively. LearnedFTL outperforms TPFTL by $1.05\times$, $1.1\times$, and $1.2\times$ under the three workloads, respectively.

4.5 Real-world Traces

We select four traces (Three WebSearch traces and one Syster trace) to evaluate the efficacy of different FTL designs. The three WebSearch traces are read-intensive workloads that are generated from a popular search engine [53]. The Syster trace is the enterprise storage traffic on modern commercial office VDI for 28 days [35, 36]. The four traces all have strong locality. For these traces, we pick the busiest periods (20 minutes to 2 hours). Since the WebSearch traces is relatively old, we re-rated 64 times more intense to reflect modern SSD workloads [39]. The workload characteristics of the four traces are summarized in Table 2. Before we replay the four traces, we warm up the whole SSD to a steady state with FIO random writes which is consistent with the previous works [39]. Since TPFTL exploits both spatial locality and temporal locality, we choose TPFTL as the baseline for the tail latency evaluation.

Figure 20 shows the *P99*, *P99.9* tail latency of TPFTL, LearnedFTL, and ideal FTL driven by the four traces. Under the four traces, compared to TPFTL, LearnedFTL reduces the *P99* tail latency by $5.3\times$, $7.4\times$, $6.5\times$, and $3.0\times$ respectively, with an average of $4.8\times$. Moreover, LearnedFTL also significantly reduces the *P99.9* tail latency of TPFTL, by up to $13.9\times$. LearnedFTL’s tail latency in WebSearch2 and WebSearch3 is extremely close to that of the ideal FTL. Although TPFTL can maintain high CMT hit ratios on workloads with

Table 2: Workload characteristics of 4 traces.

Traces	# of I/O	avg. I/O size	Read ratio
WebSearch1	1,055,235	15.5KB	100%
Websearch2	1,200,964	15.3KB	99.98%
Websearch3	793,073	15.7KB	99.96%
Systor17	1,253,423	10.25KB	61.6%

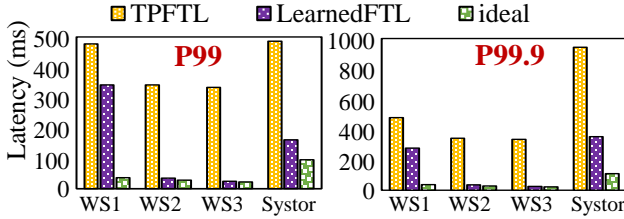


Figure 20: The tail latency results under 3 WebSearch traces (WS# demotes WebSearch#).

strong locality, sporadic double reads still induce high tail latency. By contrast, LearnedFTL’s learned model can further reduce these sporadic double reads by accurate PPN prediction, thus reducing tail latency.

5 Related Work

5.1 Mapping Schemes in FTL Design

Existing address mapping schemes in flash-based SSDs can be classified into three categories: (1) page-level mapping, (2) block-level mapping, and (3) hybrid mapping. A survey paper [42] provides a broad overview of some typical address translation technologies for flash memories [19, 25, 50, 54]. Among them, page-level mapping shows the best performance due to fine-grained mapping, but it requires a large mapping table [9, 10, 21, 44, 47, 48, 62, 63]. The existing mapping schemes share a common design principle: exploiting the workload locality to selectively cache a small part of mapping entries in DRAM while storing the whole mapping table on flash. As a result, they work well under workloads with strong access locality. However, if the working set is too large or accesses are random, the cache hit ratio will be very low and the performance will degrade significantly due to frequent swapping operations and double reads [63].

Recent studies also utilize machine learning (ML) techniques to improve the performance of flash-based SSDs [3, 26, 37, 57, 61]. For example, Q-FTL [61] uses a reinforcement learning-driven cache replacement algorithm to adapt and respond to ever-changing I/O streams, but only for specific workloads, i.e., remote sensing datasets. LearnedSSD [37] accelerates the development of new SSD devices by automating the hardware parameter configurations by utilizing both supervised and unsupervised ML techniques. Yang et al. [57] reduced GC overhead in SSD by introducing ML techniques to predict the future temperature of data. However, none of them have considered ML-based methods on the address mapping optimizations within flash-based SSDs.

5.2 Learned Index

Learned index builds an explicit model of the underlying data to provide effective indexing. It was first introduced in [31] and many learned indexes have been proposed based on the idea, such as PGM index [15], FITing tree [17], ALEX [13], Flood [46], Tsunami [14], and FINEdex [40]. They all investigate how to support update capability, provide better worst-case guarantees, and/or efficient index construction for different workloads.

Recently, BOURBON [12] shows how to integrate learned index structure for an LSM-based KV store. BOURBON employs greedy piecewise linear regression to learn key distributions and applies a cost-benefit strategy to decide when learning will be worthwhile, thus enabling fast lookup with minimal computation. APEX [41] is a PM-optimized learned index based on ALEX [13]. APEX retains the benefits of learned indexes while guaranteeing crash consistency on PM and supporting instant recovery and scalable concurrency. Abu-Libdeh et al. [1] demonstrate how a learned index can be integrated into a distributed and disk-based database system, Google’s Bigtable. Their results also validate that integrating the learned index can significantly improve the end-to-end read latency and throughput for Bigtable.

Inspired by these advancements in the learned index techniques, LearnedFTL is the first study on leveraging the learned index to improve the page-level FTL designs of flash-based SSDs to accelerate the address translation for workloads with random accesses. Different from the aforementioned learned index techniques, LearnedFTL exploits the GC characteristics of flash devices to relocate physical flash pages and a virtual PPN representation to satisfy the training requirements of the learned index. Moreover, it eliminates the error interval associated with the traditional learned index with the bitmap prediction filter to reduce read amplification in flash storage.

6 Conclusion

Applying the learned index technique to the page-level FTL designs of flash-based SSDs is non-trivial and faces the three main challenges of model selection, disordering of PPNs, and model correctness assessment. To address these challenges, we propose LearnedFTL, a learning-based page-level FTL design, by exploiting some unique characteristics of both the flash device and the learned index. LearnedFTL exploits the page relocation characteristics of GC and builds learned models to translate LPNs to their PPNs. Our FEMU-based prototype and trace-driven evaluations show that LearnedFTL reduces the P99 latency of the state-of-the-art TPFTL scheme by an average of $4.8\times$, and performs very close to the ideal FTL in both average latency and tail latency under heavy loads. Moreover, LearnedFTL also provides much better performance under other benchmark evaluations.

References

- [1] Hussam Abu-Libdeh, Deniz Altınbüken, Alex Beutel, Ed H. Chi, Lyric Doshi, Tim Kraska, Xiaozhou (Steve) Li, Andy Ly, and Christopher Olston. Learned Indexes for a Google-scale Disk-based Database. In *Proceedings of Workshop on ML for Systems at NeurIPS 2020*, pages 1–5, 2020.
- [2] Nitin Agrawal, Vijayan Prabhakaran, Ted Wobber, John D. Davis, Mark Manasse, and Rina Panigrahy. Design Tradeoffs for SSD Performance. In *Proceedings of the USENIX Annual Technical Conference (USENIX ATC’08)*, pages 57–70, 2008.
- [3] Ibrahim Umit Akgun, Ali Selman Aydin, Aadil Shaikh, Lukas Velikov, and Erez Zadok. A Machine Learning Framework to Improve Storage System Performance. In *Proceedings of the 13th ACM Workshop on Hot Topics in Storage and File Systems (HotStorage’21)*, pages 94–102, 2021.
- [4] Remzi H Arpaci-Dusseau and Andrea C Arpaci-Dusseau. *Operating Systems: Three Easy Pieces*. Arpaci-Dusseau Books LLC, 2018.
- [5] Shai Bergman, Niklas Cassel, Matias Bjørling, and Mark Silberstein. ZNSwap: un-Block your Swap. In *Proceedings of the USENIX Annual Technical Conference (USENIX ATC’22)*, pages 1–17, July 2022.
- [6] Åke Björck. Least squares methods. *Handbook of numerical analysis*, 1:465–652, 1990.
- [7] Matias Bjørling, Abutalib Aghayev, Hans Holmberg, Aravind Ramesh, Damien Le Moal, Gregory R Ganger, and George Amvrosiadis. ZNS: Avoiding the Block Interface Tax for Flash-based SSDs. In *Proceedings of the USENIX Annual Technical Conference (USENIX ATC’21)*, pages 689–703, 2021.
- [8] Yu Cai, Yixin Luo, Erich F Haratsch, Ken Mai, and Onur Mutlu. Data retention in MLC NAND flash memory: Characterization, optimization, and recovery. In *Proceedings of the 21st International Symposium on High Performance Computer Architecture (HPCA’15)*, pages 551–563, 2015.
- [9] Hao Chen, Cheng Li, Yubiao Pan, Min Lyu, Yongkun Li, and Yinlong Xu. HCFTL: A Locality-aware Page-level Flash Translation Layer. In *Proceedings of the 2019 Design, Automation & Test in Europe Conference & Exhibition (DATE’19)*, pages 590–593, 2019.
- [10] Shuo-Han Chen, Che-Wei Tsao, and Yuan-Hao Chang. Beyond Address Mapping: A User-Oriented Multiregional Space Management Design for 3-D NAND Flash Memory. *IEEE Transactions on Computer-Aided Design of Integrated Circuits and Systems*, 39(6):1286–1299, 2019.
- [11] Michael Cornwell. Anatomy of a Solid-State Drive. *Communications of the ACM*, 55(12):59–63, 2012.
- [12] Yifan Dai, Yien Xu, Aishwarya Ganesan, Ramnathan Alagappan, Brian Kroth, Andrea C. Arpaci-Dusseau, and Remzi H. Arpaci-Dusseau. From WiscKey to Bourbon: A Learned Index for Log-Structured Merge Trees. In *Proceedings of the 14th USENIX Conference on Operating Systems Design and Implementation (OSDI’20)*, pages 155–171, 2020.
- [13] Jialin Ding, Umar Farooq Minhas, Jia Yu, Chi Wang, Jaeyoung Do, Yinan Li, Hantian Zhang, Badrish Chandramouli, Johannes Gehrke, Donald Kossmann, and David Lomet. ALEX: An Updatable Adaptive Learned Index. In *Proceedings of the 2020 ACM International Conference on Management of Data (SIGMOD’20)*, pages 969–984, 2020.
- [14] Jialin Ding, Vikram Nathan, Mohammad Alizadeh, and Tim Kraska. Tsunami: A Learned Multi-dimensional Index for Correlated Data and Skewed Workloads. *Proceedings of the VLDB Endowment*, 14(2):74–86, 2020.
- [15] Paolo Ferragina and Giorgio Vinciguerra. The PGM-Index: a Fully-dynamic Compressed Learned Index with Provable Worst-case Bounds. *Proceedings of the VLDB Endowment*, 13(8):1162–1175, 2020.
- [16] Filebench. <https://github.com/filebench/filebench>, 2021.
- [17] Alex Galakatos, Michael Markovitch, Carsten Binnig, Rodrigo Fonseca, and Tim Kraska. FITing-Tree: A Data-aware Index Structure. In *Proceedings of the 2019 ACM International Conference on Management of Data (SIGMOD’19)*, pages 1189–1206, 2019.
- [18] Laura M Grupp, John D Davis, and Steven Swanson. The Harey Tortoise: Managing Heterogeneous Write Performance in SSDs. In *Proceedings of the 2013 USENIX Annual Technical Conference (USENIX ATC’13)*, pages 79–90, 2013.
- [19] Aayush Gupta, Youngjae Kim, and Bhuvan Ugaonkar. DFTL: a Flash Translation Layer Employing Demand-Based Selective Caching of Page-Level Address Mappings. In *Proceedings of the 14th International Conference on Architectural Support for Programming Languages and Operating Systems (ASPLOS’09)*, pages 229–240, 2009.

- [20] Kyuhwa Han, Hyunho Gwak, Dongkun Shin, and Jooyoung Hwang. ZNS+: Advanced Zoned Namespace Interface for Supporting In-storage Zone Compaction. In *Proceedings of the 15th USENIX Symposium on Operating Systems Design and Implementation (OSDI'21)*, pages 147–162, 2021.
- [21] Kyuhwa Han, Hyukjoong Kim, and Dongkun Shin. WAL-SSD: Address Remapping-based Write-ahead-logging Solid-State Disks. *IEEE Transactions on Computers*, 69(2):260–273, 2019.
- [22] Yang Hu, Hong Jiang, Dan Feng, Lei Tian, Hao Luo, and Shuping Zhang. Performance Impact and Interplay of SSD Parallelism through Advanced Commands, Allocation Strategy and Data Granularity. In *Proceedings of the 25th International Conference on Supercomputing (ICS'11)*, pages 96–107, 2011.
- [23] Yang Hu, Hong Jiang, Dan Feng, Lei Tian, Shuping Zhang, Jingning Liu, Wei Tong, Yi Qin, and Liuzheng Wang. Achieving Page-mapping FTL Performance at Block-mapping FTL Cost by Hiding Address Translation. In *Proceedings of the 26th Symposium on Mass Storage Systems and Technologies (MSST'10)*, pages 1–12, 2010.
- [24] Jens Axboe, Flexible I/O Tester. <https://github.com/axboe/fio>, 2022.
- [25] Song Jiang, Lei Zhang, Xinhao Yuan, Hao Hu, and Yu Chen. S-FTL: An Efficient Address Translation for Flash Memory by Exploiting Spatial Locality. In *Proceedings of the IEEE 27th Symposium on Mass Storage Systems and Technologies (MSST'11)*, pages 1–12, 2011.
- [26] Wonkyung Kang, Dongkun Shin, and Sungjoo Yoo. Reinforcement Learning-assisted Garbage Collection to Mitigate Long-tail Latency in SSD. *ACM Transactions on Embedded Computing Systems*, 16(5s):1–20, 2017.
- [27] Sudarsun Kannan, Nitish Bhat, Ada Gavrilovska, Andrea Arpaci-Dusseau, and Remzi Arpaci-Dusseau. Redesigning LSMs for Nonvolatile Memory with NovelLSM. In *Proceedings of the USENIX Annual Technical Conference (USENIX ATC'18)*, pages 993–1005, 2018.
- [28] Vamsee Kasavajhala. Solid State Drive vs. Hard Disk Drive Price and Performance Study. *Proc. Dell Tech. White Paper*, pages 8–9, 2011.
- [29] Juwon Kim, Minsu Jang, Muhammad Danish Tehseen, Joontaek Oh, and YouJip Won. IPLFS: Log-Structured File System without Garbage Collection. In *Proceedings of the USENIX Annual Technical Conference (USENIX ATC'22)*, pages 739–754, July 2022.
- [30] Youngjae Kim, Brendan Tauras, Aayush Gupta, and Bhuvan Urgaonkar. Flashsim: A Simulator for NAND flash-based Solid-State Drives. In *Proceedings of the 1st International Conference on Advances in System Simulation (SIMUL'09)*, pages 125–131, 2009.
- [31] Kraska Tim and Beutel Alex and Chi Ed H and Dean Jeffrey and Polyzotis Neoklis. The Case For Learned Index Structures. In *Proceedings of the 2018 International Conference on Management of Data (SIGMOD'18)*, pages 489–504, 2018.
- [32] Hunki Kwon, Eunsam Kim, Jongmoo Choi, Donghee Lee, and Sam H. Noh. Janus-FTL: Finding the Optimal Point on the Spectrum between Page and Block Mapping Schemes. In *Proceedings of the 10th International Conference on Embedded Software (EMSOFT'10)*, pages 169–178, October 2016.
- [33] Tomer Lange, Joseph Naor, and Gala Yadgar. Offline and Online Algorithms for SSD Management. *Proceedings of the ACM on Measurement and Analysis of Computing Systems*, 5(3):1–28, 2021.
- [34] Changman Lee, Dongho Sim, Joo-Young Hwang, and Sangyeun Cho. F2FS: A New File System for Flash Storage. In *Proceedings of the 13th USENIX Conference on File and Storage Technologies (FAST'15)*, pages 273–286, 2015.
- [35] Chunghan Lee, Tatsuo Kumano, Tatsuma Matsuki, Hiroshi Endo, Naoto Fukumoto, and Mariko Sugawara. Systor '17 Traces (SNIA IOTTA Trace Set 4928). In *SNIA IOTTA Trace Repository*. 2016.
- [36] Chunghan Lee, Tatsuo Kumano, Tatsuma Matsuki, Hiroshi Endo, Naoto Fukumoto, and Mariko Sugawara. Understanding Storage Traffic Characteristics on Enterprise Virtual Desktop Infrastructure. In *Proceedings of the 10th ACM International Systems and Storage Conference (Systor'17)*, pages 1–11, 2017.
- [37] Daixuan Li and Jian Huang. A Learning-based Approach Towards Automated Tuning of SSD Configurations. *CoRR*, abs/2110.08685, 2021.
- [38] Huaicheng Li, Mingzhe Hao, Michael Hao Tong, Swaminathan Sundararaman, Matias Bjørling, and Haryadi S Gunawi. The CASE of FEMU: Cheap, Accurate, Scalable and Extensible Flash Emulator. In *Proceedings of the 16th USENIX Conference on File and Storage Technologies (FAST'18)*, pages 83–90, 2018.
- [39] Huaicheng Li, Martin L Putra, Ronald Shi, Xing Lin, Gregory R Ganger, and Haryadi S Gunawi. IODA: A Host/Device Co-Design for Strong Predictability Contract on Modern Flash Storage. In *Proceedings of*

the 28th Symposium on Operating Systems Principles (SOSP'21), pages 263–279, 2021.

- [40] Pengfei Li, Yu Hua, Jingnan Jia, and Pengfei Zuo. FINEdex: a Fine-grained Learned Index Scheme for Scalable and Concurrent Memory Systems. *Proceedings of the VLDB Endowment*, 15(2):321–334, 2021.
- [41] Baotong Lu, Jialin Ding, Eric Lo, Umar Farooq Minhas, and Tianzheng Wang. APEX: a High-Performance Learned Index on Persistent Memory. *Proceedings of the VLDB Endowment*, 15(5):597–610, 2021.
- [42] Dongzhe Ma, Jianhua Feng, and Guoliang Li. A Survey of Address Translation Technologies for Flash Memories. *ACM Computing Surveys*, 46(3):1–39, 2014.
- [43] Stathis Maneas, Kaveh Mahdavian, Tim Emami, and Bianca Schroeder. Operational Characteristics of SSDs in Enterprise Storage Systems: A Large-Scale Field Study. In *Proceedings of the 20th USENIX Conference on File and Storage Technologies (FAST'22)*, pages 165–180, 2022.
- [44] Ronnie Mativenga, Joon-Young Paik, Youngjae Kim, Junghee Lee, and Tae-Sun Chung. RFTL: Improving Performance of Selective Caching-based Page-level FTL through Replication. *Cluster Computing*, 22(1):25–41, 2019.
- [45] Dushyanth Narayanan, Eno Thereska, Austin Donnelly, Sameh Elnikety, and Antony Rowstron. Migrating Server Storage to SSDs: Analysis of Tradeoffs. In *Proceedings of the 4th ACM European Conference on Computer Systems (EuroSys'09)*, pages 145–158, 2009.
- [46] Vikram Nathan, Jialin Ding, Mohammad Alizadeh, and Tim Kraska. Learning Multi-dimensional Indexes. In *Proceedings of the 2020 ACM International Conference on Management of Data (SIGMOD'20)*, pages 985–1000, 2020.
- [47] Fan Ni, Chunyi Liu, Yang Wang, Chengzhong Xu, Xiao Zhang, and Song Jiang. A Hash-based Space-Efficient Page-level FTL for Large-Capacity SSDs. In *Proceedings of the IEEE International Conference on Networking, Architecture, and Storage (NAS'17)*, pages 1–6, 2017.
- [48] Yubiao Pan, Yongkun Li, Huizhen Zhang, Hao Chen, and Mingwei Lin. GFTL: Group-Level Mapping in Flash Translation Layer to Provide Efficient Address Translation for NAND Flash-Based SSDs. *IEEE Transactions on Consumer Electronics*, 66(3):242–250, 2020.
- [49] R. Hugo Patterson, Garth A. Gibson, Eka Ginting, Daniel Stodolsky, and Jim Zelenka. Informed Prefetching and Caching. In *Proceedings of the 15th Symposium of Operating Systems Principles (SOSP'95)*, pages 79–95, December 1995.
- [50] Zhiwei Qin, Yi Wang, Duo Liu, and Zili Shao. A Two-level Caching Mechanism for Demand-based Page-level Address Mapping in NAND Flash Memory Storage Systems. In *Proceedings of the 17th IEEE Real-Time and Embedded Technology and Applications Symposium (RTAS'11)*, pages 157–166, 2011.
- [51] Pandian Raju, Rohan Kadekodi, Vijay Chidambaram, and Ittai Abraham. Pebblesdb: Building Key-Value Stores Using Fragmented Log-structured Merge Trees. In *Proceedings of the 26th Symposium on Operating Systems Principles (SOSP'17)*, pages 497–514, 2017.
- [52] RocksDB. <https://github.com/facebook/rocksdb>, 2022.
- [53] UMass Trace Repository. University of Massachusetts Amherst. <https://traces.cs.umass.edu/index.php/Storage/Storage>, 2014.
- [54] Mingbang Wang, Youguang Zhang, and Wang Kang. ZFTL: A Zone-based Flash Translation Layer with a Two-tier Selective Caching Mechanism. In *Proceedings of the 14th International Conference on Communication Technology (ICCT'12)*, pages 578–588, 2012.
- [55] Shucheng Wang, Ziyi Lu, Qiang Cao, Hong Jiang, Yuanguan Dong, and Puyuan Yang. BCW: Buffer-Controlled Writes to HDDs for SSD-HDD Hybrid Storage Server. In *Proceedings of the 18th USENIX Conference on File and Storage Technologies (FAST'20)*, pages 253–266, 2020.
- [56] Xingda Wei, Rong Chen, and Haibo Chen. Fast RDMA-based ordered key-value store using remote learned cache. In *Proceedings of the 14th USENIX Conference on Operating Systems Design and Implementation*, pages 117–135, 2020.
- [57] Pan Yang, Ni Xue, Yuqi Zhang, Yangxu Zhou, Li Sun, Wenwen Chen, Zhonggang Chen, Wei Xia, Junke Li, and Kihyoun Kwon. Reducing Garbage Collection Overhead in SSD based on Workload Prediction. In *11th USENIX Workshop on Hot Topics in Storage and File Systems (HotStorage'19)*, pages 1–6, 2019.
- [58] Ting Yao, Yiwen Zhang, Jiguang Wan, Qiu Cui, Liu Tang, Hong Jiang, Changsheng Xie, and Xubin He. MatrixKV: Reducing Write Stalls and Write Amplification in LSM-tree Based KV Stores with Matrix Container in NVM. In *Proceedings of the USENIX Annual Technical Conference (USENIX ATC'20)*, pages 17–31, 2020.

- [59] Sangjin Yoo and Dongkun Shin. Reinforcement Learning-Based SLC Cache Technique for Enhancing SSD Write Performance. In *Proceedings of the 12th USENIX Workshop on Hot Topics in Storage and File Systems (HotStorage'20)*, 2020.
- [60] Jiacheng Zhang, Jiwu Shu, and Youyou Lu. ParaFS: A Log-structured File System to Exploit the Internal Parallelism of Flash Devices. In *Proceedings of the USENIX Annual Technical Conference (USENIX ATC'16)*, pages 89–100, June 2016.
- [61] Tong Zhang, Ze Cheng, and Jing Li. Reinforcement Learning-driven Address Mapping and Caching for Flash-based Remote Sensing Image Processing. *Journal of Systems Architecture*, 98(c):374–387, 2019.
- [62] Jian Zhou, Dezhi Han, Jun Wang, Xiaobo Zhou, and Changjun Jiang. A Correlation-aware Page-Level FTL to Exploit Semantic Links in Workloads. *IEEE Transactions on Parallel and Distributed Systems*, 30(4):723–737, 2018.
- [63] You Zhou, Fei Wu, Ping Huang, Xubin He, Changsheng Xie, and Jian Zhou. An Efficient Page-level FTL to Optimize Address Translation in Flash Memory. In *Proceedings of the 10th European Conference on Computer Systems (EuroSys'15)*, pages 1–16, 2015.
- [64] You Zhou, Qiulin Wu, Fei Wu, Hong Jiang, Jian Zhou, and Changsheng Xie. Remap-SSD: Safely and Efficiently Exploiting SSD Address Remapping to Eliminate Duplicate Writes. In *Proceedings of the 19th USENIX Conference on File and Storage Technologies (FAST'21)*, pages 187–202, 2021.